Hindawi
Geofluids
Volume 2022, Article ID 1069471, 9 pages
https://doi.org/10.1155/2022/1069471

WILEY | Hindawi

Research Article

Diffraction Wave Attributes to Identify Small-Scale Geological Bodies

Mengcheng Shu

China University of Petroleum, Beijing 102249, China

Correspondence should be addressed to Mengcheng Shu; shumch@geobutton.com.cn

Received 15 March 2022; Accepted 24 May 2022; Published 27 June 2022

Academic Editor: Di Feng

Copyright © 2022 Mengcheng Shu. This is an open access article distributed under the Creative Commons Attribution License, which permits unrestricted use, distribution, and reproduction in any medium, provided the original work is properly cited.

Aiming at the difficulties in the fine description of small- and medium-scale geological bodies in storage, this paper develops a method for describing geological bodies using diffracted wave data and systematically explains the effectiveness of the method through model calculations. Finally, this method is applied to fractures. In the fine description of the type of reservoir and the intrusive rock mass of the reservoir, two diffraction wave attribute analysis methods are used to achieve the fine description of the distribution law of the above small-scale geological bodies. The principal component analysis method is proposed to extract the diffraction from the seismic wave field. Information, the wave field is separated through the kinematics and dynamics of the diffraction wave, and the obtained diffraction wave field better reflects the distribution law of small-scale geological bodies. Verified by examples, the diffraction wave analysis method can be more refined and a comprehensive description of the distribution of small-scale geological bodies.

1. Introduction

With the deepening of global oil and gas field exploration, the fine description of medium- and small-scale reservoirs has gradually become a key issue for oilfield exploration. The identification of fracture and vug spaces in carbonate reservoirs (Zhang, 2008; Qian, 2008), especially the identification of fractured reservoirs (Murray, 1968; Ruger, 1997; Neves, 2004; Ai-Dossary, 2004; Shen, 2002; Gray, 2000; Hall, 2003; Schoenberg, 1999) has received widespread attention. The conventional reflection wave reservoir description method is limited by the wave field resolution, and it is difficult to describe this kind of geological body finely [1].

Previous studies have confirmed that the diffraction wave field can be better described for small-scale geological bodies (Gallop & Hron, 1998; Klem-Musatov, 2008; Taner, 2006; Zhu, 2010; Ivan et al., 2013); when the spatial scale of the local geological body is close to or smaller than the resolution of seismic reflection data (generally less than $\lambda/4$), the diffraction wave data separated from the seismic data can be used to finely describe small-scale geological bodies. Therefore, the predecessors according to the dynamics and wave characteristics of the diffraction wave field, different diffraction wave extraction methods are proposed (Xie, 2021; Liang, 2019). The calculation efficiency of the prestack diffraction wave extraction method is low, which is not conducive to the rapid development of the reservoir. Recognition, the poststack diffraction wave extraction method has become an important means of reservoir identification, so the paper proposes a diffraction wave attribute extraction method based on principal component analysis technology, while considering the dynamics and kinematics of the seismic wave field, separates it from the seismic wave field diffraction waves, and proposes a diffraction wave attribute analysis method for different geological problems, so as to achieve a fine description of the distribution of small-scale geological bodies [2–4].

2. Materials and Methods

2.1. Poststack Diffraction Wave Extraction Method Based on Principal Component Analysis Technology

2.1.1. Diffraction Wave Generation. According to the Huygens principle, in the process of seismic wave propagation,

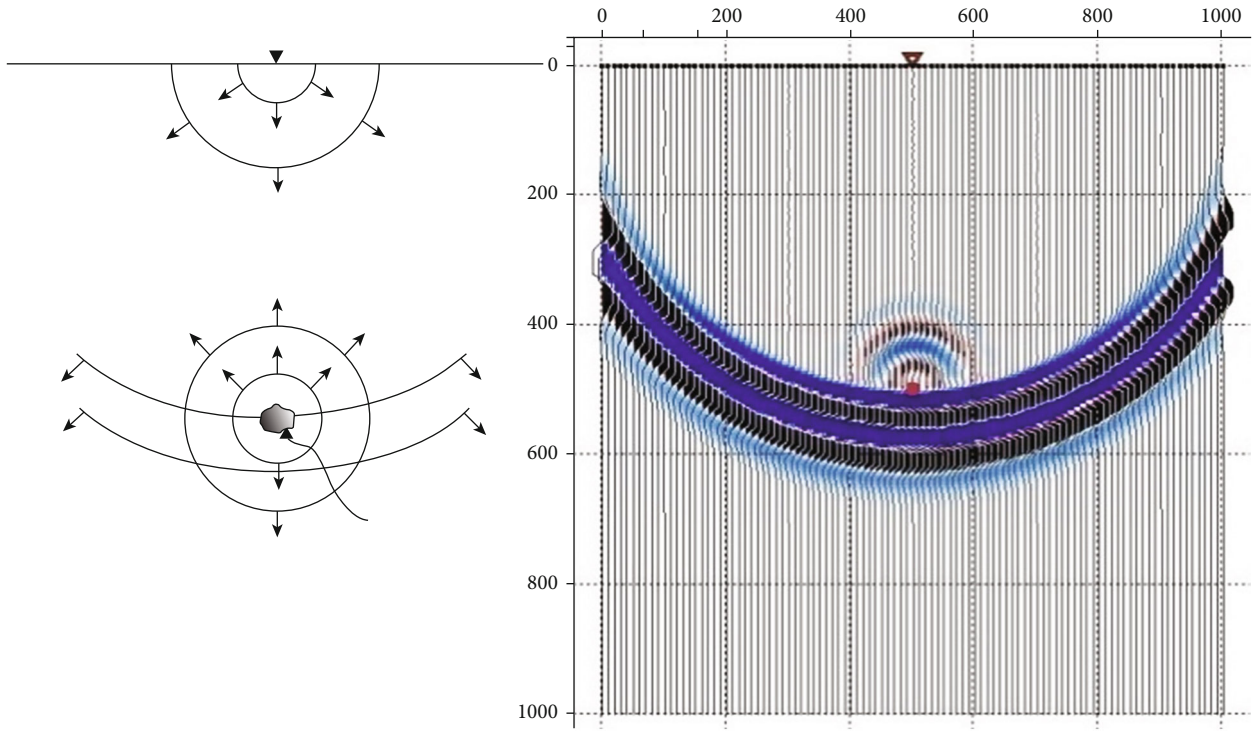

Figure 1: The generation of diffracted wave (Li, 2012).

in addition to generating a reflected wave, some seismic waves related to complex structures will also be generated. Points, protrusions on unconformity surfaces will generate new seismic sources, reemit spherical waves, propagate to the surroundings, and form diffracted waves in seismic exploration (as shown in Figure 1).

2.1.2. Poststack Diffraction Wave Extraction Method. The idea of extracting the poststack diffracted wave is mainly to identify the difference between the amplitude and phase characteristics of the diffracted wave and the reflected wave after the superposition or migration of the diffracted wave and to separate the diffraction information. This paper is based on the kinematics and dynamics of the diffracted wave in the poststack seismic data features (Shu, 2014), using principal component analysis technology to extract diffraction wave information.

Generally, principal component analysis (PCA) is used in multiscale analysis, data dimensionality reduction and compression, etc.; in the article, it is applied to the separation of reflected waves and diffracted waves, through the characteristics of the difference in amplitude of the two waves and the difference in spatial distribution. Perform wave field separation [5].

The PCA algorithm can sort the target data into mutually orthogonal data volumes, and the sorting basis is how much these data volumes contribute to the total variance. The calculation of the three-dimensional autocorrelation function is actually the calculation of the correlation factors between different data volumes. The size of the data volume is the same, but there is a certain displacement along different directions (the main survey line, the contact survey line, and the depth direction). The core of the PCA algorithm is shown in

$$\Lambda = \Phi^T C \Phi, \tag{1}$$

where C is the covariance matrix of the multidimensional vector X. In this article, C is the three-dimensional autocorrelation function of the calculated data volume, Φ is the eigenvector of C, and Λ is the eigenvalue matrix.

For the calculation of three-dimensional data volume, formula (1) is improved (as shown in formula (2)). The orthogonal data volume corresponding to different feature vectors can be calculated, the characteristics of different wave fields can be separated according to this, and the geology of different scales can be realized by the purpose of the body description.

$$O_{ijk}^r = \frac{\lambda^r}{MNL} \sum_{m=1}^{M} \sum_{n=1}^{N} \sum_{l=1}^{L} \tilde{S}_{mnl}^r \tilde{\Phi}_{mnl}^r, \tag{2}$$

$$\tilde{S}_{mnl}^r = \frac{S_{mnl}^r - \mu}{\sigma}. \tag{3}$$

In the formula, O_{ijk}^r is the r orthogonal component of the calculation matrix, and the central calculation point is i, j, and k; S_{mnl}^r and $\tilde{S}_{mnl}^r$ are the calculation matrices before and after standardization, respectively; n, m, and l are the spatial position of the offset matrix involved in the calculation; N,

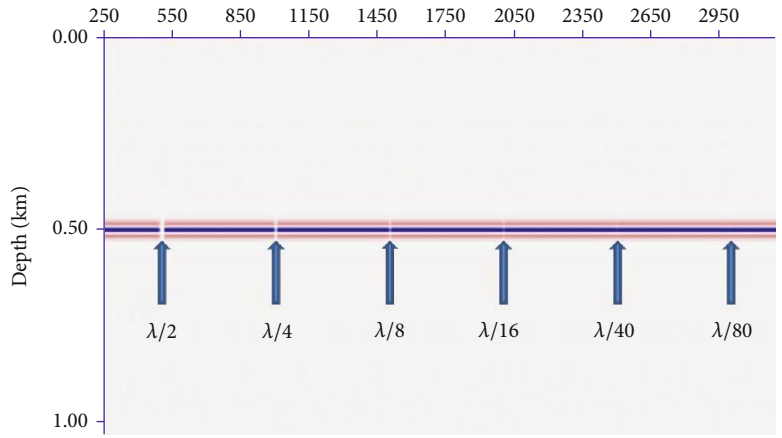

Figure 2: Forward model of the lens of different lateral scales.

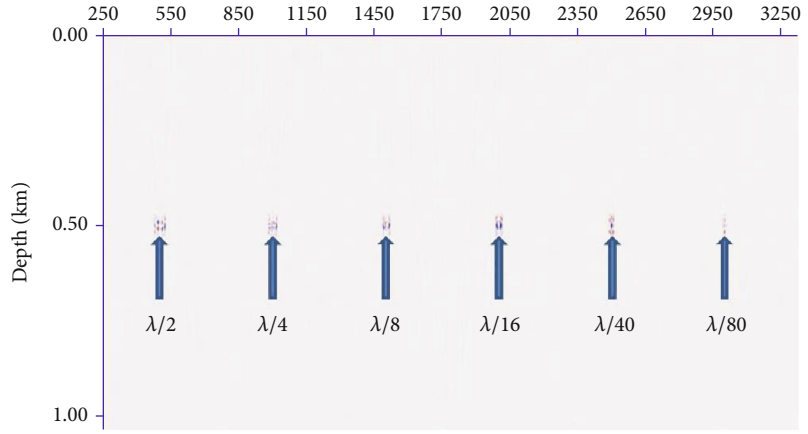

Figure 3: Forward model of the diffracted wave of different lateral scales.

M, and L are the number of offset matrices in different directions; μ is the mean value of the sample amplitude in the calculated matrix; σ is the standard deviation of the sample amplitude in the calculated matrix; λ^r is the matrix eigenvalue; $\tilde{\Phi}^r_{mnl}$ is the diagonal matrix of Φ^r_{mnl}.

The new coordinate axis after transformation is the direction of each feature vector, and the data volume of different principal components can be obtained by corresponding coordinate conversion of the original data volume. Because the energy of the diffraction wave is much smaller than the energy of the reflected wave (about the reflected wave 1/100 of the energy), so in the analysis, it is necessary to analyze the characteristics of the diffraction wave in the low-order components [6, 7].

2.2. Diffraction Characteristic Analysis. In this paper, lens models of different spatial scales are established, and the resolution ability of diffracted waves on small-scale anomalies is analyzed through the width and thickness of the lens. The model parameters are as follows: longitudinal wave speed: 2 km/s; wavelet dominant frequency: 25 Hz; wavelength: 80 m; buried depth of lens: 1 km.

This section discusses the ability of the diffracted wave to recognize the lens when the horizontal width of the lens changes.

It can be seen from Figures 2 and 3 that for the diffraction profile of the low-noise lens, the diffraction wave can identify the horizontal width of $\lambda/16$ (5 meters), and the boundary of the lens can be distinguished. The width is $\lambda/40$ and $\lambda/80$; it is already difficult to identify the position of the lens on the reflection offset profile, but through the extraction of diffraction information, the spatial position of this tiny lens can still be described more clearly [8–10].

When it is assumed that the lateral width of the lens is the smallest (without considering the change of the lateral event axis), this section gives the diffraction response of the lens model with different vertical thickness changes and analyzes the resolution ability of the diffraction wave. Figures 4 and 5 show the offset profile and the corresponding diffraction wave extraction profile at different vertical thicknesses. The model parameters are as follows: longitudinal wave speed: 2 km/s; wavelet dominant frequency: 25 Hz; wavelength: 80 m.

As shown in Figures 4 and 5, when the lens body has a large thickness and is easy to identify (the lens body vertical

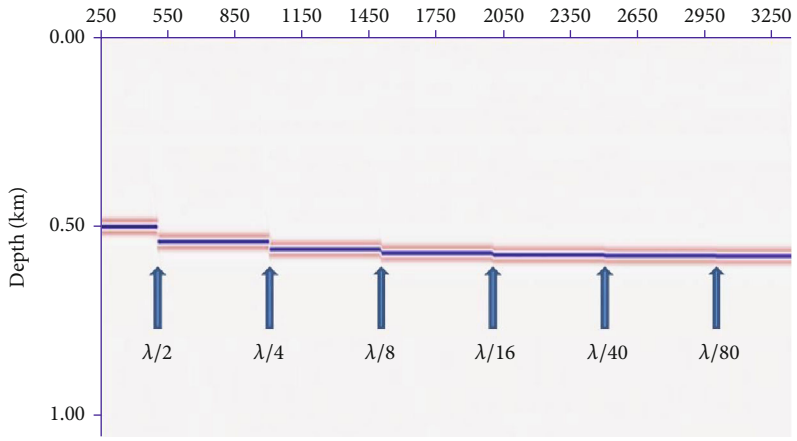

Figure 4: Forward model of the lens of different vertical scales.

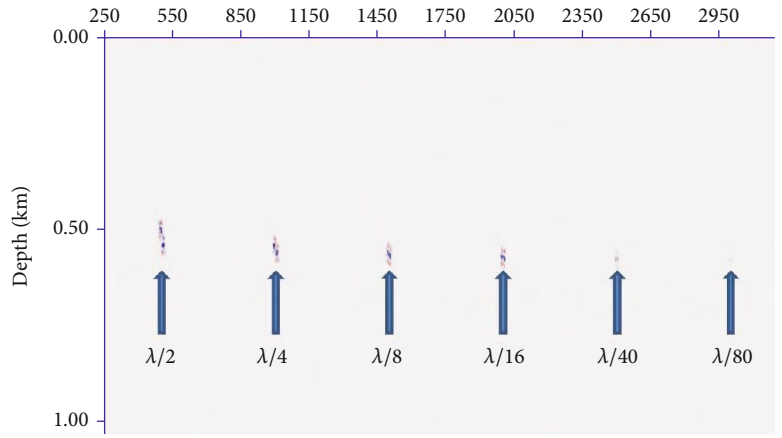

Figure 5: Forward model of the diffracted wave of different vertical scales.

thickness > $\lambda/8$), the extracted diffraction information can well describe the spatial distribution characteristics of the lens body; when the size of the lens is very small and it is difficult to recognize artificially (the vertical thickness of the lens < $\lambda/8$), it can be seen from the extracted diffraction profile that the position of the lens is still a more accurate description that can be obtained, until the thickness of the lens body is close to the point diffraction (as shown in Figure 6); the diffraction wave profile response is close to the point diffraction response [11–13].

3. Results and Discussion

3.1. Small-Scale Intrusive Rock Characterization. The distribution characteristics of intrusive rocks in carbonate reservoirs are difficult to identify. If the intrusive position is close to the top of the reservoir, the intrusive rock and the top of the reservoir will form wave field interference, and it is difficult to effectively identify this part of the intrusive rock with conventional attributes. The diffraction wave extraction technology can effectively separate the diffraction wave field caused by the intrusive rock from the reflected wave field on the top of the carbonate reservoir and finally achieve the purpose of fine description of the spatial distribution of the intrusive rock [14, 15].

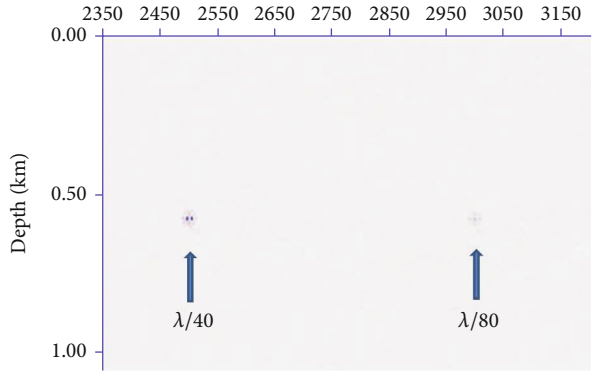

Figure 6: The local section of the small-scale lens model.

In this paper, the diffraction information of the experimental area is extracted, and the results are compared with the conventional reflected wave attribute extraction results. As shown in Figures 7 and 8, the drilling results of this area (Well C, Well D, and Well E) reveal the reservoirs in the target area. It is very developed, and the along-layer attributes

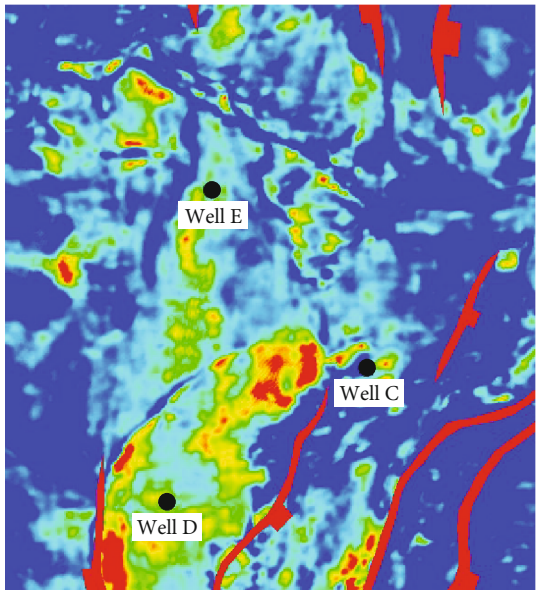

Figure 7: RMS attribution of the P-wave of RMS prediction map of igneous distribution.

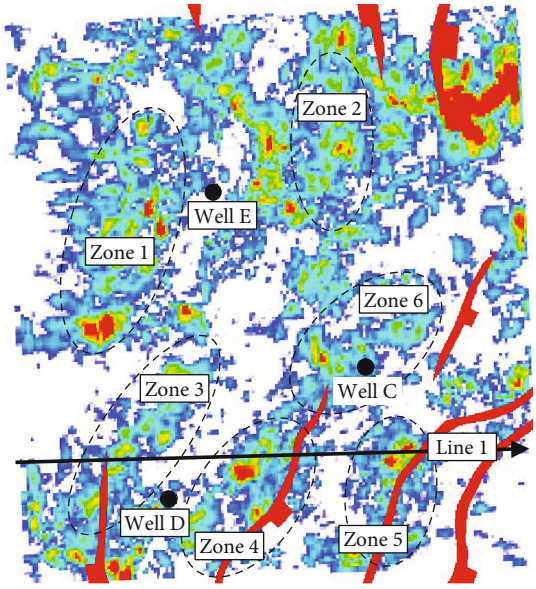

Figure 8: RMS attribution of the diffracted wave of RMS prediction map of igneous distribution.

extracted from the reflected wave data volume can better reflect the distribution law of the reservoir. However, Well C and Well D both encountered intrusive rocks, and the intrusive rocks drilled by Well C were separated from the top surface of the reservoir at only 18 m; conventional attributes cannot describe these two intrusive rocks (Figure 7).

It can be seen from Figure 8 that the along-layer attributes extracted from the diffraction wave data can well eliminate the influence of reservoir distribution characteristics and reflect the spatial distribution of intrusive rocks and faults, that is, Well C and Well D in the reservoir section. Intrusive rocks are developed, and Well E has complete reservoir characteristics. At the same time, in order to eliminate the ambiguity of the diffraction wave attribute analysis method and to distinguish the diffraction wave response of faults and intrusive rocks, the paper combines the results of fault interpretation with seismic reflection data. Analyze the energy distribution area of the diffraction wave generated by the fault through the corresponding relationship between the fault position and the diffraction energy, so as to isolate the distribution law of the intrusive rock mass [16–18].

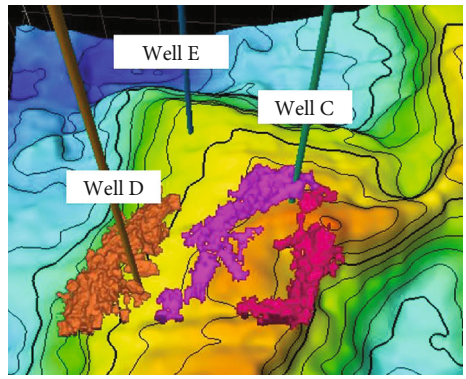

Figure 9: The igneous geobody beside Well C and Well D.

Two seismic sections are selected for analysis in this paper (as shown in Figure 8). Line 1 passes through two abnormal areas (Zone 1 and Zone 2). From the analysis in Figure 9, it can be seen that these two energy distribution areas are fault development locations. Although they are associated faults, they are small in scale. Diffraction waves show such faults. The RMS attribute map shows that the energy is relatively concentrated at the breakpoint and presents a strip-like plane distribution [19, 20].

Line 2 has passed through three diffraction anomaly regions (Zone 3, Zone 4, and Zone 5). From Figure 8, we can see that the three anomalous regions have a good correlation with the deep and large faults explained by reflection data, and the faults are developed. The location, although it is an associated fault, is small in scale. The diffraction wave shows the features of this type of fault, which shows that the energy is concentrated at the breakpoint and shows a strip-like planar distribution. By comparison, in Figure 8, it can also be seen that the spatial distribution of the fault is in good agreement with the attribute distribution of the diffracted wave [21–23].

Based on the above analysis, this paper divides the study into 6 diffractive wave field development areas and summarizes the structural interpretation scheme of the diffraction wave development area and the reflected wave field, as well as the comparison of drilling results (as shown in Table 1).

The analysis of Table 1 shows that Well D revealed that Zone 3 developed intrusive rocks and developed fault diffraction, indicating that there is an associated relationship between intrusive rocks and fault-developed areas, and deep and large faults may become the intrusion methods and paths of volcanic intrusive rocks. It is necessary to analyze whether other fault diffractions may also contain intrusive rocks [24, 25].

Table 1: The diffracted wave attribute of igneous compared with fault interpretation and logging result.

	Zone 1	Zone 2	Zone 3	Zone 4	Zone 5	Zone 6
Fault	√	√	√	√	√	
Drilling reveals intrusive rocks			√			√

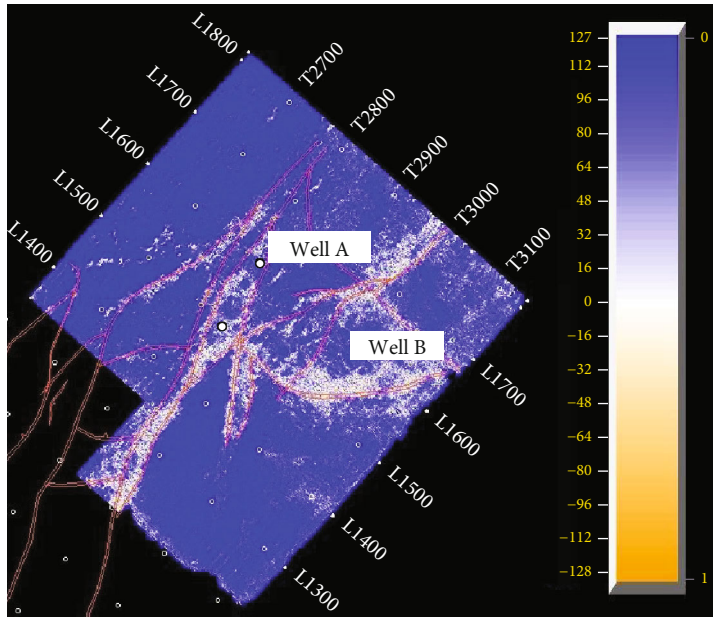

Figure 10: The map of RMS attribute based on diffraction data.

In this paper, a method of applying volcanic intrusive rock space engraving is proposed, and the relationship between the distribution law of intrusive rock mass and deep and large faults is analyzed through the spatial connectivity characteristics of diffraction wave data.

Because the volcanic intrusive rock satisfies the regional continuous distribution characteristics in terms of geological genesis, the continuous distribution of diffraction energy is extracted from the diffraction wave attribute data volume for volume carving. The analysis can obtain (1) the fault and well predicted by Zone 3 in Figure 9. The intrusive rock encountered by drill D (the grey area in the figure) has a very good accompanying relationship; (2) the black part in the figure (corresponding to Zone 4-Zone 6) is the main body of intrusive rock continuously distributed, indicating the magmatic rock at Well C, the feature of intruding into the reservoir through a fault and limited development in the reservoir.

3.2. Characterization of the Small-Scale Fracture System. In this paper, a buried hill fracture development area is selected for the study of fracture properties. The study area is the Archean oil-bearing strata, mainly composed of mixed granite and migmatite; as an example of the application of the comprehensive method, the effect analysis of the method application is carried out [26, 27].

The diffraction wave information crack detection technology is used to target the top surface of the buried hill, and the root mean square amplitude attribute is selected to describe the crack distribution in the target area, and the crack density prediction result is obtained (as shown in Figure 10, the white is the high-density distribution area of cracks). Based on the diffraction wave data volume, the crack space is extracted, and the ant tracking method is selected to obtain the prediction result of the crack orientation (as shown in Figures 11 and 12).

For structural fracture type oil and gas reservoirs, the fractures are mainly distributed in locations with strong structural deformation. As can be seen from the figure, the extracted diffraction waves are mainly distributed on both sides of the near-fault surface of the structural deep fault, which is nearly parallel to the deep fault. This area has strong structural deformation and relatively developed fractures. According to the results revealed by drilling, the prediction results of diffraction fractures can better describe the distribution of fractures in the work area [28, 29].

The results obtained by the fracture azimuth prediction method are in good agreement with the drilling encounter results of known wells. At the same time, the fracture prediction results in the area near the wellbore also reflect that for Well A, the fracture distribution at the wellbore location is mainly south-east-NW and south-south-east-NW, and the fracture distribution plan of the diffracted wave shows that the overall trend of the fracture distribution is in line with the fracture distribution law encountered by the borehole; for Well B, the fracture distribution at the borehole location

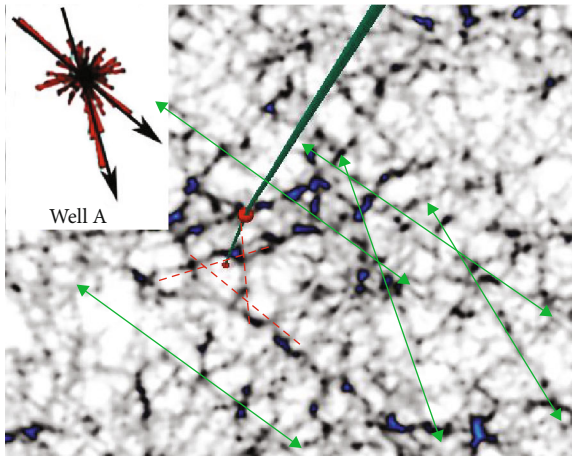

Figure 11: Prediction map of Well A of the fracture azimuth predicted result compared with imaging log.

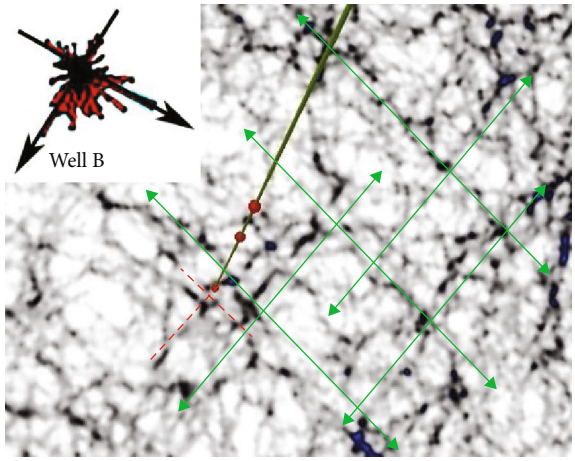

Figure 12: Prediction map of Well B of the fracture azimuth predicted result compared with imaging log.

is mainly the prediction results of the diffracted wave crack azimuth can also reflect this distribution law.

Through section comparison, relatively continuous reflection events can be distinguished in the reflection section. For conventional structural interpretation work, only larger-level faults can be explained, and the spatial distribution of the fracture system cannot be described. It can be seen in the fracture prediction profile of radio wave information that due to stable deposition, an event axis with stable spatial distribution of amplitude will be formed, so using the fracture prediction and extraction method of diffraction wave information, this part of the event axis is effectively suppressed; for example, the target area of the fracture distribution area (due to the regional anisotropy caused by the distribution of fractures, the diffraction wave in this area is relatively developed, and the spatial stability of the reflected wave amplitude is poor.) will retain the diffraction waves generated by the fracture system [29, 30]. The spatial distribution of this part of the diffraction wave extracted by the fracture corresponds to the spatial distribution area of the fracture, which is the information related to the fracture system that is difficult to distinguish in the reflection profile.

After the diffraction information is extracted from the poststack data, the ant tracking method is used to describe the crack distribution results. Comparing the automatic tracking results of reflected and diffracted cracks, it can be seen that the large-scale faults predicted based on the reflection data are suppressed in the diffraction prediction results. The small-scale fracture system is prominent. It can also be seen from the superimposed map that the predicted fractures are densely distributed in the central and eastern part of the profile (the area with complex structures) [31–35], while the predicted fractures in the western part of the profile (the event axis continuous area) are not developed. And the fracture distribution zone extracted and predicted by diffraction information has a certain similarity with the spatial distribution of the buried mountain surface.

4. Conclusions

(1) A method for extracting the diffraction wave field of poststack seismic data is proposed in the article. The forward model of the diffraction wave proves that the diffraction wave data extracted by this method can recognize small-scale geological bodies up to 1/40 wavelength, which proves the effectiveness of the poststack diffraction wave extraction method

(2) Aiming at the problem of fracture identification in fractured oil and gas reservoirs, the paper proposes to use the diffraction wave method to extract characteristic attributes, finally gives the results of the fracture density distribution and azimuth prediction through the targeted thinking, and verifies the effectiveness of the method through drilling data

(3) Aiming at the problem of identifying intrusive rock bodies in carbonate reservoirs, the article analyzes in detail the idea of separation of intrusive rock diffraction wave fields, proposes a research method for predicting the spatial distribution of intrusive rocks, and finally gives the well-controlled range of intrusive rock bodies. The spatial distribution characteristics of the drilling data are used to verify the effectiveness of the method

Data Availability

All data included in this study are available upon request by contact with the corresponding author.

Conflicts of Interest

The authors declare no conflict of interest.

Acknowledgments

We gratefully acknowledge the China University of Petroleum and the Strategic Cooperation Technology Projects of CNPC and CUPB (ZLZX2020-03) for the financial support and the Strategic Priority Research Program (Category A) of Chinese Academy of Sciences: Velocity Modelling and Reservoir Prediction Techniques with logging and seismic while drilling (XDA14040301).

References

[1] Z. H. Hong, Z. H. Junmao, Y. A. Daoqing, Y. A. Chunfeng, C. H. Bingzhang, and Z. H. Chi, "Prediction of paleokarst reservoir in the south eastern slope of Tazhong area in Tarim Basin using seismic techniques," *Acta Petrolei Sinica*, vol. 29, no. 1, pp. 69–74, 2008.

[2] Q. Rongjun, *Characteristics of Seismic Waves and Related Technical Analysis*, Petroleum Industry Press, Beijing, 2008.

[3] S. Ai-Dossary, Y. Simon, and K. J. Marfurt, "Inter azimuth coherence attribute for fracture detection," *SEG Technical Program Expanded Abstracts*, vol. 23, pp. 183–186, 2004.

[4] J. B. Gallop and F. Hron, "Diffractions and boundary conditions in asymptotic ray theory," *Geophysical Journal International*, vol. 133, no. 2, pp. 413–418, 1998.

[5] D. Gray, "Fracture detection in Manderson field: a 3-D AVAZ case history," *The Leading Edge*, vol. 19, no. 11, pp. 1214–1221, 2000.

[6] S. A. Hall and J. M. Kendall, "Fracture characterization at Valhall: application of P-wave amplitude variation with offset and azimuth (AVOA) analysis to a 3D ocean-bottom data set," *Geophysics*, vol. 68, no. 4, pp. 1150–1160, 2003.

[7] P. Ivan and S. Aaron, "Fracture detection through seismic cube orthogonal decomposition," *SEG Annual Meeting*, pp. 1308–1313, 2013.

[8] K. D. Klem-Musatov, A. M. Aizenberg, J. Pajchel, and H. B. Helle, *Edge and Tip Diffractions Theory and Applications in Seismic Prospecting*, SEG, 2008.

[9] G. H. Murray, "Quantitative fracture study–Sanish pool, Mckenzie County, North Dakota," *AAPG Bulletin*, vol. 52, no. 1, pp. 57–65, 1968.

[10] F. A. Neves, M. S. Zahrani, and S. W. Bremkamp, "Detection of potential fractures and small faults using seismic attributes," *TLE*, vol. 23, no. 9, pp. 903–906, 2004.

[11] A. Rüger, "P-wave reflection coefficients for transversely isotropic models with vertical and horizontal axis of symmetry," *Geophysics*, vol. 62, no. 3, pp. 713–722, 1997.

[12] M. A. Schoenberg, S. Dean, and C. M. Sayers, "Azimuth-dependent tuning of seismic waves reflected from fractured reservoirs," *Geophysics*, vol. 64, no. 4, pp. 1160–1171, 1999.

[13] F. Shen, J. Sierra, D. Burns, and M. N. Toksoz, "Azimuthal offset-dependent attributes (AVO AND FVO) applied to fracture detection," *SEG Technical Program Expanded Abstracts*, vol. 18, no. 1, pp. 776–785, 1999.

[14] M. T. Taner, *Prestack Separation of Seismic Diffractions Using Plane-Wave Decomposition*, SEG, Expanded Abstracts, 2006.

[15] X. S. Zhu and R. S. Wu, "Imaging diffraction points using the local image matrices generated in prestack migration," *Geophysics*, vol. 75, no. 1, pp. S1–S9, 2010.

[16] X. Wei, B. I. Chen-Chen, H. Hua-feng, M. Yong-qiang, M. Ling-wei, and Y. Ming, "Development and application of an identification method for fracture and cave in carbonate reservoir based on diffracted wave," *Science Technology and Engineering*, vol. 21, no. 2, pp. 453–457, 2021.

[17] L. Zhiqiang, "Poststack seismic prediction techniques for fractures of different scales," *Geophysical Prospecting for Petroleum*, vol. 58, no. 5, pp. 766–772, 2019.

[18] L. Xueliang, *Diffraction Wave Imaging and Its Application in Fracture Prediction*, Institute of Geology and Geophysics, Chinese Academy of Sciences, Beijing, 2012.

[19] S. Mengcheng, *Comprehensive Description Method of Fracture-Cavity Reservoirs*, Institute of Geology and Geophysics, Chinese Academy of Sciences, Beijing, 2014.

[20] Z. Liang and L. Xue, "Weak signal seismic identification technology based on reflected wave separation," *Natural Gas Exploration and Development*, vol. 3, pp. 22–26, 2021.

[21] P. S. Rowbotham, "Realization of wave field separation by three-dimensional filtering in interwell seismic reflection processing," *Petroleum Geophysical Translation Cong*, vol. 2, pp. 36–39, 1995.

[22] W. Jing, Q. Niannian, and C. Fei, "Reverse time migration reflected wave suppression method and comparative analysis," *Journal of Engineering Geophysics*, vol. 4, pp. 43–46, 2013.

[23] S. K. Lazaratos, "Interwell high-resolution imaging of carbonate reservoirs in West Texas: part 4: reflected wave imaging," *Petroleum Geophysical Translation Cluster*, vol. 2, pp. 28–31, 1996.

[24] W. Mengqian, Y. Jianhua, and L. Shengdong, "Reflected wave advance imaging forecasting system and its application," *Advances in Geophysics*, vol. 3, pp. 23–26, 2014.

[25] L. Cai, D. Shixue, Y. Baojun, and T. Dayi, "Application of polarization filtering in separation of P and S wave fields for wide-angle earthquakes," *Geophysical and Geochemical Calculation Technology*, vol. 2, pp. 41–45, 1995.

[26] L. Zhiming, J. F. Claerbout, and R. A. Ottolini, "Migration of flipped reflected waves by bidirectional extrapolation," *Petroleum Geophysical Prospecting*, vol. 1, pp. 20–22, 1985.

[27] C. Daxiong, "Reflection-reflection wave," *Acta Geophysics*, vol. 4, pp. 32–36, 1965.

[28] C. Zhuang, "Reverse time migration imaging of mine reflected wave advance detection," *Inner Mongolia Coal Economy*, vol. -Z2, pp. 28–31, 2017.

[29] H. Jianwei, D. Yong, D. Dun, P. Hailong, F. Zhongyu, and J. Fenghua, "Double-detection signal wavefield separation based on non-Gaussian maximization in undulating sea surface environment," *Petroleum Geophysical Exploration*, vol. 4, pp. 29–32, 2018.

[30] L. Cai, D. Shixue, Y. Baojun, and T. Dayi, "Application of polarization filtering in separation of P and S wave fields of wide-angle earthquakes," *Geophysical and Geochemical Exploration Computing Technology*, vol. 2, pp. 33–36, 1995.

[31] Z. Simeng, H. Liguo, and Y. Chenxia, "Reverse time migration bidirectional illumination wave field separation imaging conditions," *World Geology*, vol. 2, pp. 44–47, 2017.

[32] L. Xueyi, C. Jiubing, W. Tengfei, G. Jianhua, and L. Yuzhu, "Wavefield separation method for seabed multicomponent seismic data with low signal-to-noise ratio," *Acta Geophysics*, vol. 2, pp. 56–59, 2021.

[33] L. Wang Mingfang and W. Y. Yunlong, "Application of high-resolution radon transform in wavefield separation of array acoustic logging," *Logging Technology*, vol. 4, pp. 66–68, 2014.

[34] L. Jun, S. Ying, and Y. Chunying, "Vector wave field separation and application in anisotropic media," *Acta Geophysics*, vol. 8, pp. 55–58, 2018.

[35] S. Hongyan, "The idea of wave field separation and denoising in seismic exploration," *Western Prospecting Engineering*, vol. 3, pp. 44–47, 2012.